Published online 10 April 2013 *Nucleic Acids Research, 2013, Vol. 41, No. 10* **5263–5272**
doi:10.1093/nar/gkt249

Mechanism of DNA organization by *Mycobacterium tuberculosis* protein Lsr2

Yuanyuan Qu[1,2,3], Ci Ji Lim[1,2,3,4], Yixun R. Whang[1,2,3], Jun Liu[5,*] and Jie Yan[1,2,3,4,*]

[1]Department of Physics, National University of Singapore, Singapore 117542, Singapore, [2]Centre for Bioimaging Sciences, National University of Singapore, Singapore 117546, Singapore, [3]Mechanobiology Institute, National University of Singapore, Singapore 117411, Singapore, [4]NUS Graduate school for Integrative Sciences and Engineering, Singapore 119077, Singapore and [5]Department of Molecular Genetics, University of Toronto, Toronto, Ontario M5S 1A8, Canada

Received January 14, 2013; Revised March 18, 2013; Accepted March 20, 2013

ABSTRACT

Bacterial nucleoid-associated proteins, such as H-NS-like proteins in Enterobacteriaceae, are abundant DNA-binding proteins that function in chromosomal DNA organization and gene transcription regulation. The *Mycobacterium tuberculosis* Lsr2 protein has been proposed to be the first identified H-NS analogue in Gram-positive bacteria based on its capability to complement numerous *in vivo* functions of H-NS. Here, we report that Lsr2 cooperatively binds to DNA forming a rigid Lsr2 nucleoprotein complex that restricts DNA accessibility, similar to H-NS. On large DNA, the rigid Lsr2 nucleoprotein complexes can mediate DNA condensation into highly compact DNA conformations. In addition, the responses of Lsr2 nucleoprotein complex to environmental factors (salt concentration, temperature and pH) were studied over physiological ranges. These results provide mechanistic insights into how Lsr2 may mediate its gene silencing, genomic DNA protection and organization functions *in vivo*. Finally, our results strongly support that Lsr2 is an H-NS-like protein in Gram-positive bacteria from a structural perspective.

INTRODUCTION

Bacterial nucleoid-associated proteins (NAPs) are small and high-copy number DNA-binding proteins involved in global gene transcription regulation and chromosomal DNA organization (1–3). They typically mediate these functions through site-specific/non-specific DNA binding and organizing DNA into various conformations (2,4). Competitions among NAPs for DNA-binding sites are believed to be regulated by their populations in cells (1,5), and regulation of individual NAP population is often controlled by themselves or by other NAPs, as shown in the case of *Escherichia coli* H-NS and StpA (6).

The *E. coli* H-NS plays critical roles as a global gene silencer and a chromosomal DNA organizer (7). It especially silences genes that are responding to environmental changes (8,9) and also laterally acquired foreign genes (10). H-NS-like proteins, which are often defined by their capabilities to complement H-NS-deficient mutants in *E. coli* (11,12), are widely spread in Gram-negative bacteria, such as StpA in *E. coli* (13), MvaT in *Pseudomonas aeruginosa* (14), BpH3 in *Bordetella pertussis* (15) and VicH in *Vibrio cholera* (16). Although these proteins are often dissimilar to each other at the sequence level, they usually exhibit similar overall structure consisting of a C-terminus DNA-binding domain and an N-terminus domain that mediates protein–protein interaction (14,17–19). In solution, H-NS-like proteins exist as dimers or higher-ordered oligomers depending on solution condition and protein concentration, which are believed important for their functions (14,20,21). Although H-NS-like proteins were widespread among Gram-negative bacteria, such proteins were much less reported in Gram-positive bacteria. Up to date, the only proposed H-NS-like protein in Gram-positive bacteria is Lsr2 in *Mycobacterium tuberculosis*, based on its capability to complement phenotypes related to H-NS mutations in *E. coli* (11). Lsr2 and H-NS also use the same DNA recognition mechanism to preferentially bind to AT-rich DNA (22).

The NAP DNA-binding mode is the mechanical basis of how they organize DNA into various conformations. For example, the *E. coli* NAP H-NS protein is able to bridge DNA to form DNA hairpins and loops at high magnesium conditions (>5 mM) (23,24), and H-NS

*To whom correspondence should be addressed. Tel: +65 65162620; Fax: +65 67776126; Email: phyyj@nus.edu.sg
Correspondence may also be addressed to Jun Liu. Tel: +416 9465067; Fax: +416 9786885; Email: jun.liu@utoronto.ca

The authors wish it to be known that, in their opinion, the first two authors should be regarded as joint First Authors.

DNA-bridging mode is proposed to be important for H-NS DNA compaction (23) and gene regulation function (23,25). Another DNA-binding mode of H-NS, DNA-stiffening mode via rigid nucleoprotein filament formation at low magnesium conditions (0–2 mM), is shown to be critical for H-NS gene-silencing functions (24,26,27). The *E. coli* NAP integration host factor (IHF) DNA-bending mode allows it to bring transcription factors closer to mediate gene regulation (28). In addition, at high protein concentration and magnesium concentration in millimolar range, IHF can mediate DNA cross-linking (29). Therefore, to understand how Lsr2 mediates its various biological functions, it is important to know Lsr2 DNA-binding mode and its dependency on environmental factors. Although Lsr2 was shown to bridge DNA using atomic force microscopy (AFM) imaging method (30), a more thorough investigation using a combination of single-molecule manipulation and imaging techniques is necessary to obtain a comprehensive picture of Lsr2 DNA-binding mode(s). The power of such combination has been demonstrated in the cases of H-NS (24), StpA (31) and MvaT (21) as compared with previous AFM imaging studies that only revealed their DNA-bridging properties (23,32).

In this work by magnetic tweezers and AFM, we show that the *M. tuberculosis* Lsr2 protein binds to DNA through a highly cooperative process resulting in an increase in apparent DNA-bending rigidity, similar to H-NS. In addition, Lsr2-induced DNA folding was also observed. The rigid Lsr2–DNA complex was also found to be stable across physiological environmental changes (salt, pH and temperature). This is more prominent in the case of magnesium salt, an important co-factor in numerous biological processes, where the rigid Lsr2–DNA complex is stable at physiological range of $MgCl_2$ concentration, whereas for comparison, the *E. coli* H-NS loses its DNA-stiffening ability and favours DNA bridging at >5 mM $MgCl_2$ (24). We also demonstrate that the Lsr2–DNA complex strongly restricts DNA accessibility, a property that is shown in H-NS *E. coli* paralogue, StpA (31). In summary, our work shows that Lsr2 has an intricate DNA-binding mode that encompasses DNA stiffening and DNA folding, which provides us a mechanistic platform in understanding how Lsr2 mediates its biological functions *in vivo*.

MATERIALS AND METHODS

Overexpression and purification of Lsr2

pET expression vector containing the *lsr2* gene was expressed according to previous protocol (30). The expressed Lsr2 protein has a C-terminal His-tag to aid protein purification.

Magnetic tweezers experiments

The magnetic tweezers set-up used in this study was similar to ones used in our previous studies (24,31,33). A single λ-DNA (48 502 bp, NEB), modified with biotin at both ends, was tethered between a streptavidin-functionalized surface and a streptavidin-coated 2.8-μm magnetic bead (Dynabeads M-270 Streptavidin, Invitrogen). The single DNA molecule extension measurement was collected in real-time (100 Hz) using a camera-based centroid tracking software written in LabVIEW program (National Instruments, USA). This set-up was previously used to measure changes in DNA rigidity caused by either DNA-stiffening proteins (24) or DNA-bending proteins (29).

Atomic force microscopy imaging

All AFM imaging experiments were done on glutaraldehyde-coated mica surface, which prevents the non-specific aggregation of proteins or DNA–protein complexes because the glutaraldehyde molecules are covalently bound to the surface. Preparation of glutaraldehyde-coated mica was done according to previous established protocols (24,31,34,35). In all AFM experiments, linearized φX174 DNA (5386 bp, NEB, USA) was used as the DNA template and incubated with the stated Lsr2 concentration or DNA/protein ratio for 20 min in 10 mM Tris–HCl and 50 mM KCl, pH 7.5, buffer condition before depositing on the glutaraldehyde-coated mica. The Lsr2 protein bound on the DNA interacts with the glutaraldehyde-coated mica surface to form covalent bonds, thus trapping the Lsr2/DNA complexes on the mica surface without the aid of divalent salts. The sample was then rinsed with deionised water and dried with a clean stream of nitrogen gas before using it for air AFM imaging. Typical AFM image scan size is 1–4 μm^2 with a scan speed of 1–2 line per second.

RESULTS

Lsr2 cooperatively binds to extended DNA and stiffens DNA

DNA-distorting proteins can modify the micromechanics property of DNA and affect its force response. Different types of DNA-distorting proteins cause different DNA force responses, which can be measured by single-DNA stretching experiments (36). Previous AFM experiments revealed that Lsr2 could bridge DNA into DNA hairpins and loops (30); however, it is unclear how Lsr2 initially interacts with an extended DNA before DNA folds, which provides the physical basis for subsequent DNA organization. Further, understanding of the property of Lsr2 on extended DNA will also provide important insights into its gene regulatory function. Therefore, we implemented a quick force-jump measurement that is able to measure the force response of DNA while preventing DNA folding during the measurement (26). This quick force-jump measurement is performed by initially holding the DNA at a high force (~20 pN), which prevents DNA folding, then jumping to a lower force for ~1 s to measure the end-to-end distance of DNA (i.e. DNA extension) before jumping back to the high force. As the DNA is only held at lower forces for very short duration, the level of DNA folding occurred at the lower forces is negligible. Repeating this process for a series of lower forces in the range of 0.3–16 pN, a force-extension curve is obtained, which quantifies the

DNA force response without interference from DNA folding.

Figure 1A shows the force-extension curves obtained by force-jumping of a λ-DNA (48 502 bp) with increasing Lsr2 concentration in 10 mM Tris–HCl and 50 mM KCl, pH 7.5, buffer condition. At each Lsr2 concentration and each force, this force-jump procedure was repeated three times to get the average values (data points) and the standard deviations (error bars) of the extensions. At 6 nM Lsr2 concentration, the DNA force response is similar to that of the naked DNA, suggesting few Lsr2 binding to DNA, which causes negligible change in the force response of DNA. Increasing Lsr2 concentration to 60 nM, the DNA extension becomes longer than that of the naked DNA, which indicates the increase of the DNA rigidity (36). Further increasing Lsr2 concentration to 600 nM makes the DNA more extended and increasing to 2400 nM only gives a slight increase in DNA extension compared with the extension in 600 nM Lsr2, which means the stiffening effect is largely saturated by 600 nM Lsr2. Here, we emphasize that the DNA stiffening caused by Lsr2 is not because of steric interaction of overcrowded Lsr2 on DNA. An example is that the *E. coli* IHF, a DNA-bending protein that binds to DNA as individual heterodimers, does not cause DNA stiffening even at over saturated IHF concentrations (29). More directly, significant DNA stiffening by Lsr2 occurred before binding saturation (e.g. at 60 nM).

The effect of Lsr2 on the DNA-bending rigidity can be quantified by fitting the measured force-jump force-extension curves with the curves predicted by the worm-like chain (WLC) polymer model of DNA (37), which only depends on the contour length and the DNA-bending rigidity described by a parameter called the DNA-bending persistence length. For a naked DNA, this parameter has been measured to be ~50 nm in physiological solution conditions (37,38). Figure 1B shows the bending persistence lengths A and contour lengths L at different Lsr2 concentrations C fitted by the Marko–Siggia formula (inset in Figure 1B). The effective contour length is nearly constant over the Lsr2 concentration range of 0–2400 nM, whereas the effective persistence length increases drastically from ~50 nm at 0 nM Lsr2 to ~490 nm at 2400 nM Lsr2. These results reveal that Lsr2 binding does not change the DNA native structure (otherwise one would expect change in the effective contour length); however, it restricts DNA bending resulting in DNA stiffening.

As only the bending persistence length is affected by Lsr2 binding, the fraction of DNA bound with Lsr2 α (occupation fraction) can be quantified by the following equation $\alpha = \left(\sqrt{1/A_{measured}} - \sqrt{1/A_{naked}}\right)/\left(\sqrt{1/A_{saturated}} - \sqrt{1/A_{naked}}\right)$ (see Supplementary Method: Derivation of Occupation Fraction Formula). The occupation fraction obtained at different Lsr2 concentrations allows us to calculate the dissociation constant k_d to be ~58 nM and the Hill coefficient n to be ~2.3 by fitting to the Hill equation $\alpha = 1/[(k_d/C)^n + 1]$ (Figure 1C) (39). The aforementioned result reveals that Lsr2 binds to extended DNA at nanomolar affinity. A greater than one Hill coefficient indicates that Lsr2 cooperatively binds to DNA. The cooperative nature can be explained by Lsr2 polymerizing along DNA to form a filamentous structure, similar to H-NS family proteins in Gram-negative bacteria (21,24,31). Here, one should notice that the DNA is forced to be in an extended conformation in the force-jump DNA stretching experiments; therefore, these values are not directly comparable with values obtained by the conventional electrophoretic mobility shift assay (EMSA). For example, k_d of 1 μM was reported by EMSA before (40), which is ~20 times the k_d value measured in our force-jump experiments. Our own EMSA result yielded similar k_d value of 1.7 μM (Supplementary Figure S1), indicating the observed k_d difference is unlikely that of a variation in protein batch activity. This difference suggests that Lsr2 may bind with higher affinity to highly extended DNA under force, which is reasonable because DNA-stiffening proteins theoretically would prefer binding to extended DNA conformations (36).

The rigid Lsr2–DNA complex condenses under low force

Previous AFM experiments revealed that Lsr2 could fold large DNA into hairpins and higher order conformations on freshly cleaved mica surface (30). Our independent AFM imaging results are consistent with the previous findings. Figure 2A shows AFM images of naked linearized double-stranded φX174 DNA (5386 bp) on glutaraldehyde-modified mica surface, which exhibits random coiled conformation. At an Lsr2 monomer to DNA base pair ratio of 1:1 (Lsr2 concentration of 300 nM), DNA is typically folded into highly complex Lsr2–DNA condensates consisting of large compact globular nucleoprotein structures (white arrows) and extended thick DNA bundles (red arrows) as shown in Figure 2B. At a lower Lsr2 monomer to DNA base pair ratio of 1:10 (Lsr2 concentration of 30 nM), the Lsr2–DNA complex typically has an Lsr2-rich core with higher height (yellow arrow) surrounded by large naked DNA loops (Figure 2C). More representative images can be found in Supplementary Data (Supplementary Figure S2).

As the results in the previous section have demonstrated that Lsr2 can cooperatively bind to extended DNA, which stiffens DNA, an interesting question raised here is whether a preformed rigid extended Lsr2 nucleoprotein structure at high force can fold when the force is dropped to lower values in single-DNA stretching experiments. Figure 2D shows the force-extension curves obtained in a force-decrease scan (red solid squares) followed by a force-increase scan (red open squares) through the same set of force values of a λ-DNA with 600 nM Lsr2 concentration in 10 mM Tris–HCl and 50 mM KCl, pH 7.5, solution condition. At each force, the DNA was held for 30 s, and extension average over this period is plotted in Figure 2D as a data point. Different from the previous force-jump, this force-scan procedure allowed DNA folding, as the DNA was held at lower forces for much longer duration.

If DNA folding was to occur during the force-decrease scan at the lower force range, non-overlapping force-extension curves (i.e. hysteresis) between the

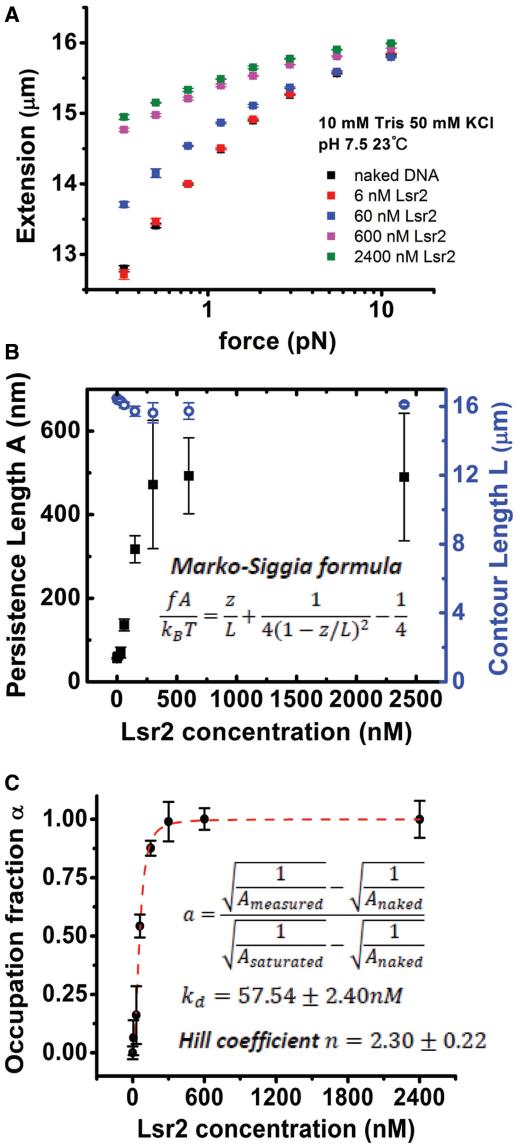

Figure 1. Cooperative formation of rigid Lsr2 nucleoprotein filament on extended 48 502 bp λ-DNA. (**A**) Force-jump force-extension curves of DNA incubated with varying Lsr2 concentrations, which shows significant DNA stiffening. The error bar at each force is given by three successive force-jump experiments on the same DNA. (**B**) The bending persistence lengths A (black solid square) and the contour lengths L (blue open circle) at different Lsr2 concentrations C of the resulting extended Lsr2–DNA complex fitted according to the Marko–Siggia formula (inserted formula). Here, f denotes the stretching force and z denotes the DNA extension. The error bar at each concentration is given by at least three independent measurements on different DNAs. At saturation (2400 nM Lsr2), A and L are determined to be 489 ± 152 nm and 16 109 ± 94 nm. (**C**) The fraction of DNA occupied by Lsr2 was calculated according to the apparent bending persistence length (see inserted formula). Its dependency on Lsr2 concentration reveals high-binding affinity and cooperativity with k_d of 57.54 ± 2.40 nM and Hill coefficient of 2.30 ± 0.22.

force-decrease and force-increase scans would be expected, which indeed occurred (Figure 2D). The DNA extension obtained in the force-decrease scan is overall longer than the naked DNA, indicating formation of rigid nucleoprotein structure at higher force range; although the shorter than naked DNA extension obtained in the subsequent force-increase scan indicates DNA folding at lower forces. Progressive DNA-folding time trace in the force range 0.08–0.18 pN was shown in the inset of Figure 2D. The folded Lsr2–DNA complex is extremely stable, which can withstand 20 pN over the experimental time scale of 20 min (Supplementary Figure S3). Overall, the folding of rigid Lsr2–DNA complexes at low force is consistent with the folded Lsr2–DNA complexes observed in AFM imaging.

The results shown in this section suggest that DNA stiffening by Lsr2 at initial binding stage does not exclude DNA folding. This is similar to MvaT, where the formation of rigid MvaT nucleoprotein filament was reported to precede and mediate MvaT-dependent DNA folding (21).

The effects of salt, pH and temperature changes to Lsr2–DNA organization properties

Formation of the rigid nucleoprotein filamentous structures has been shown universal in H-NS-like proteins and critical for their gene-silencing functions in Gram-negative bacteria (21,24,26,27,31). The formation of the H-NS-like nucleoprotein filaments by those proteins was often regulated by environmental factors, such as salt concentrations, pH value and temperature (21,24,26,27,31). As Lsr2 has been proposed to be the first H-NS-like protein in Gram-positive bacteria (11), and it also forms rigid nucleoprotein structure on extended DNA by cooperative DNA binding, we now focus on how environmental factors affect the formation of the Lsr2 nucleoprotein structure on the extended DNA.

As Lsr2 can simultaneously stiffen and fold DNA, two sets of experiments were conducted to separately investigate the effects of the environmental factors on these two Lsr2–DNA-binding modes. To investigate the effects on the DNA-stiffening property, force-jump procedure described in the previous section was performed to prevent DNA folding (Figure 3A–D). Then a force-scan (force decrease scan followed by force increase scan) experiment was conducted to probe the effects on the DNA-folding property (Figure 3E–H).

Previous study showed that the function of DNA protection against hydroxyl radical damage of Lsr2 depends on salt concentration, and it lost the function in 800 mM NaCl buffer condition (41). Here, we show that at 800 mM KCl concentration, Lsr2 at 600 nM is unable to form the rigid nucleoprotein structure on extended DNA (Figure 3A), indicated by no changes in the force-extension curves between the naked DNA (blue solid squares) and the same DNA after Lsr2 was introduced (yellow solid squares). DNA folding did not occur either in the force-scan procedure (Figure 3E). Similar results were obtained at 2400 nM Lsr2, suggesting that at 800 mM KCl, Lsr2 fails to stably bind to DNA at micromolar concentration range (Supplementary Figure S4). On the same DNA and at the same Lsr2 concentration of 600 nM, DNA stiffening was observed when the force-jump experiments were repeated in lower KCl concentrations of 300, 150 and 50 mM, successively (Figure 3A). The DNA

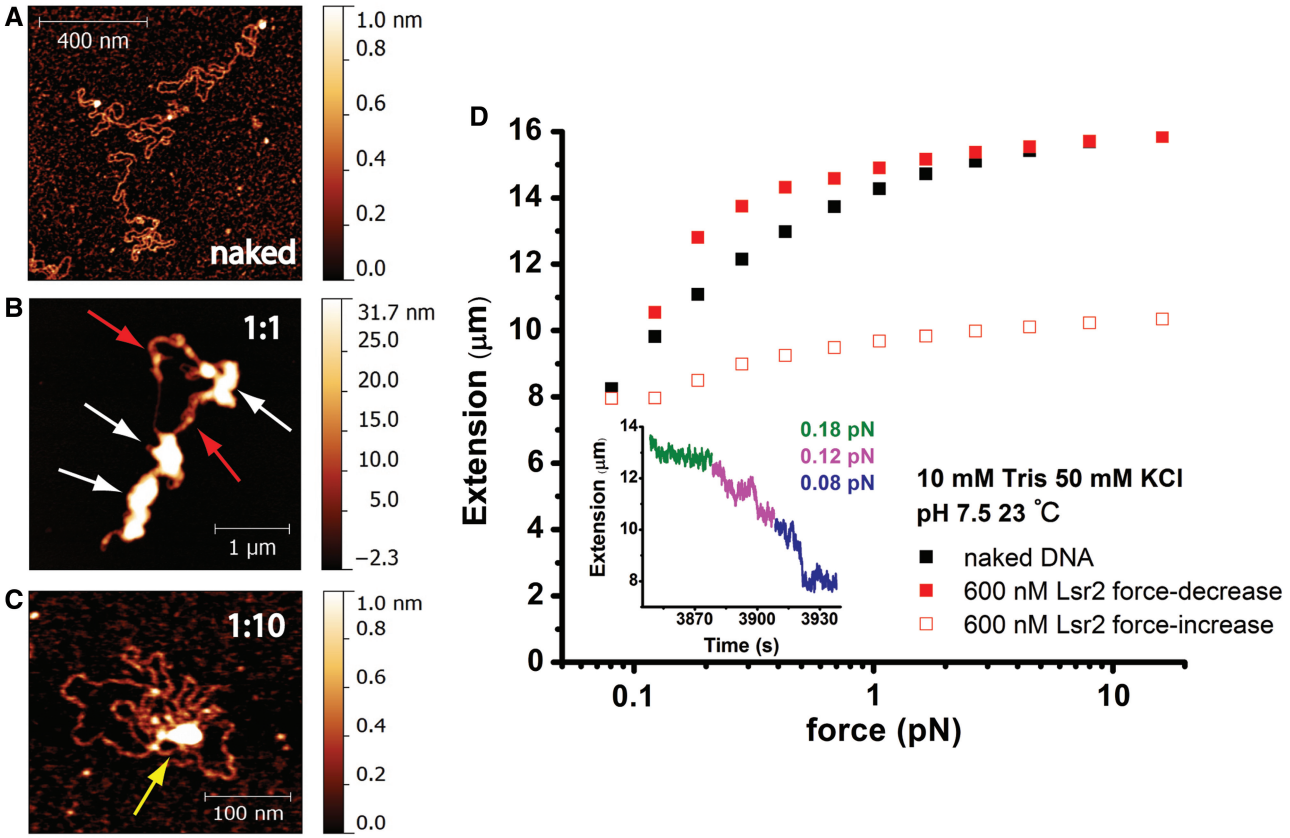

Figure 2. The rigid Lsr2–DNA complex condenses under low force. (**A–C**) AFM images show typical random coiled naked linearized 5386-bp φX174 DNA (A), typical Lsr2–DNA complexes consisting of large condensates (white arrows) and extended thick DNA bundles (red arrows) at an Lsr2 monomer to DNA bp ratio of 1:1 (B), and typical Lsr2–DNA complexes consisting of Lsr2-riched cores (yellow arrow) surrounded by large naked DNA loops at a lower Lsr2 monomer to DNA base pair ratio of 1:10 (C). More images can be found in Supplementary Data (Supplementary Figure S1). (**D**) Force-extension curves obtained by a force-decrease scan (red solid squares) followed by a force-increase scan (red open squares) through the same set of force values of a λ-DNA at 600 nM Lsr2 concentration in 10 mM Tris–HCl and 50 mM KCl, pH 7.5. Inset shows progressive DNA folding at small force (<0.2 pN). The non-overlapping force-extension curves between the force-decrease and force-increase scans indicate the mixed effects of DNA stiffening and DNA folding.

became increasingly stiffer as KCl concentration was decreased, suggesting the formation of rigid Lsr2–DNA complex in lower KCl concentrations. Similarly, folding was also observed when lowering the KCl concentration (Figure 3E), indicated by the hysteric force-extension curves between the force-decrease and force-increase scans.

Previous studies on *E. coli* H-NS have shown that the capability to form rigid nucleoprotein filaments is reduced at higher magnesium concentration. At 10 mM $MgCl_2$, the *E. coli* H-NS in μM range of concentration is unable to stiffen DNA (23,24,32). In contrast, other H-NS family proteins, such as StpA and MvaT, are able to form rigid nucleoprotein filaments insensitively to magnesium concentration of the same range (21,31). Figure 3B shows that the force-jump curves obtained with 600 nM Lsr2 in 0, 1, 4 and 10 mM $MgCl_2$ all overlap, indicating that the formation of rigid Lsr2 nucleoprotein structure is insensitive to 0–10 mM $MgCl_2$, similar to StpA and MvaT. Additionally, DNA folding still occurs under low forces in 0–10 mM $MgCl_2$ in the force-scan procedure (Figure 3F).

Similar studies were performed to investigate the effects of temperature (Figure 3C and G) and pH (Figure 3D and H). DNA stiffening by Lsr2 was found moderately tuned by temperature (Figure 3C). At the human body temperature of 37°C, significant reduction in the DNA-stiffening effect of Lsr2 was observed, which is also observed in *E. coli* H-NS (24). This effect can be explained by either a disruption in Lsr2 DNA-stiffening ability or a reduction in Lsr2 DNA-binding affinity at 37°C, such as in the case of high-salt buffer conditions. In contrast, the DNA-stiffening effect by Lsr2 was found insensitive to pH values ranging from 6.8 to 8.8, unlike the highly pH sensitive *E. coli* H-NS (24). We also showed the DNA-folding effect by Lsr2 is not sensitive to changes in buffer temperature (Figure 3G) or pH value (Figure 3H), as DNA folding can always be induced in all the conditions explored under low forces.

These results suggest that despite the disruption of rigid Lsr2–DNA nucleoprotein complex under high-salt condition (800 mM KCl) and the moderate reduction in the Lsr2–DNA-stiffening effect at the human body temperature; the Lsr2–DNA complex is a robust structure not sensitive to physiological range of changes in environmental conditions.

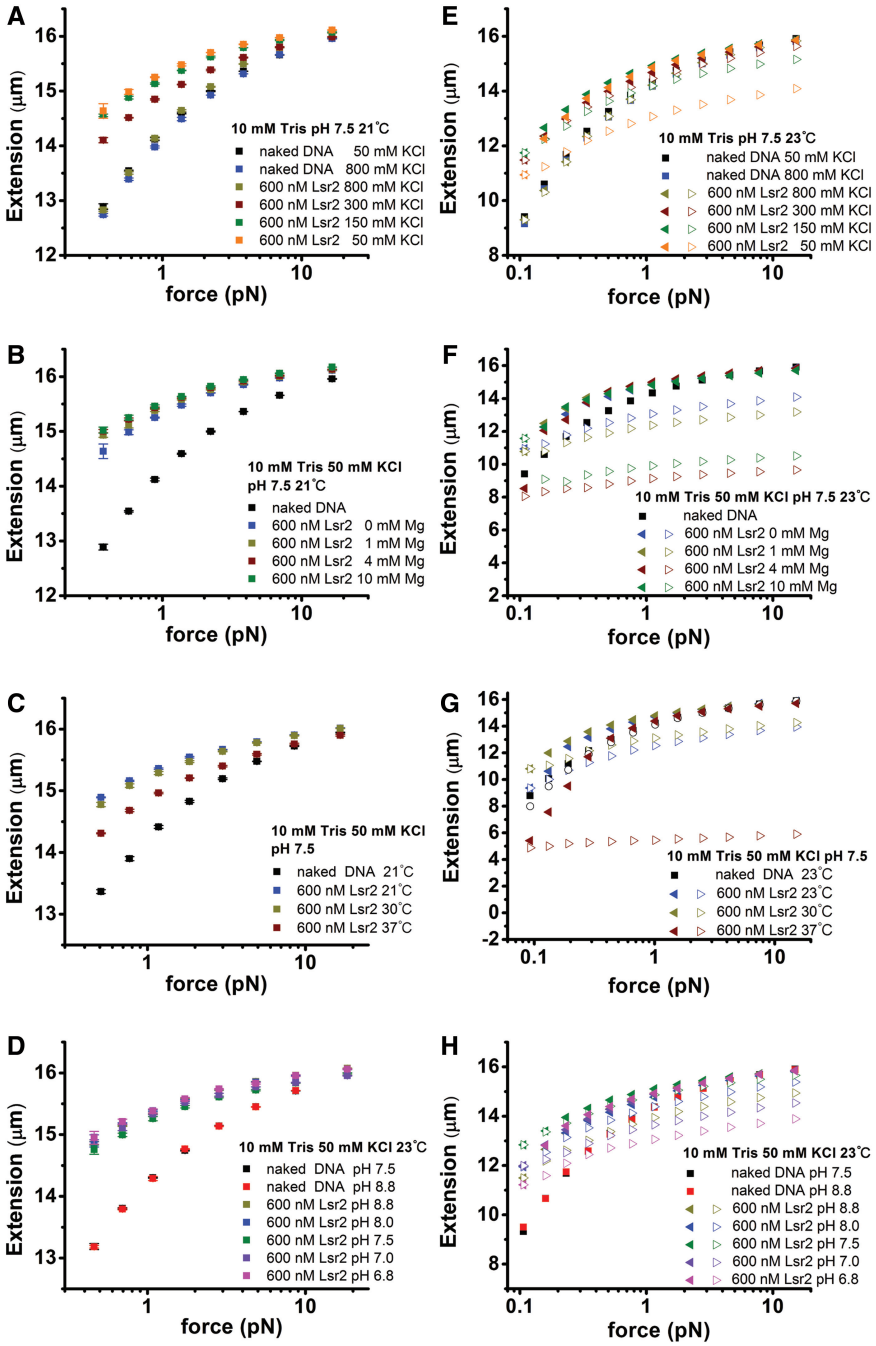

Figure 3. Effects of environmental factors on rigid Lsr2 nucleoprotein structure formation at 600 nM Lsr2. Force-jump force-extension curves (**A**–**D**) and force-scan force-extension curves (**E**–**H**) of Lsr2–DNA complex are plotted separately with decreasing KCl concentration (**A**, **E**), increasing magnesium concentration (**B**, **F**), increasing temperature (**C**, **G**) and decreasing pH value (**D**, **H**). Eight independent λ-DNA tethers were used to obtain data in the eight panels. In the force-scan force-extension panel (E–H), the solid left triangles represent the force decrease scan, whereas the open right triangles represent the force increase scan. Different colours indicate different experimental conditions. Overall, level of DNA stiffening is negatively regulated by increasing KCl concentration or temperature, whereas it is insensitive to $MgCl_2$ concentration or pH value over the range explored in experiments. The DNA-folding effect by Lsr2 is always observed in all conditions explored in experiments.

The rigid Lsr2–DNA complex is able to restrict access to DNA

Previous biochemical study has already demonstrated that Lsr2–DNA complexes are resistant to DNase I digestion (40). As Lsr2 can form rigid nucleoprotein structure on extended DNA, which also mediates higher level of DNA condensation, it is unclear whether the DNA protection from DNase I digestion in that experiment is due to DNA condensation, or the formation of the Lsr2–DNA nucleoprotein structure alone is sufficient for DNA protection. Therefore, in this section, we examine the level of restriction of the accessibility to extended DNA covered by Lsr2.

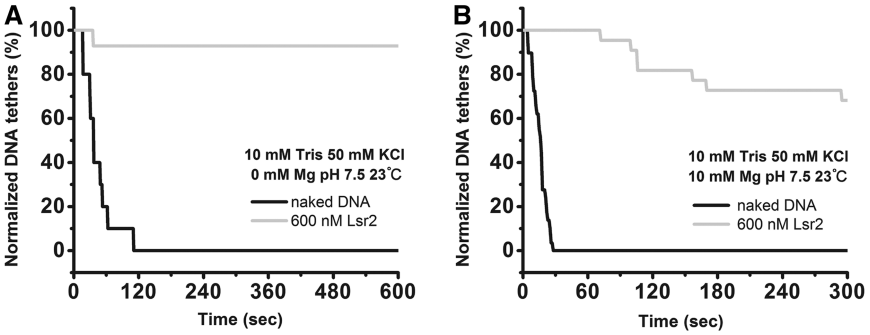

Figure 4. DNase I digestion assays of DNA accessibility restriction by rigid Lsr2–DNA complex formed on extended DNA. (**A**) Normalized survival DNA tethers of 10 unprotected naked DNA (black) by 200 nM DNase I in 50 mM KCl or 14 pre-formed rigid Lsr2–DNA complex tethers with 600 nM Lsr2 (light grey) by 200 nM DNase I in 50 mM KCl. (**B**) Normalized survival DNA tethers of 22 unprotected naked DNA (black) by 200 nM DNase I in 50 mM KCl and 10 mM $MgCl_2$ or 29 pre-formed rigid Lsr2–DNA complex tethers with 600 nM Lsr2 (light grey) by 200 nM DNase I in 50 mM KCl and 10 mM $MgCl_2$. In both reaction buffer conditions, compared with the unprotected naked DNAs, formation of the rigid Lsr2–DNA complex on extended DNA drastically slows down the DNA digestion rate.

By using a multiplex detection algorithm developed in our previous study (31), dozens of DNA tethers were stretched at ~10 pN and monitored at the same time. In all, 600 nM of Lsr2 protein was introduced in 10 mM Tris–HCl and 50 mM KCl, pH 7.5, in the absence of $MgCl_2$ (Figure 4A) or in the presence of 10 mM $MgCl_2$ (Figure 4B), to allow formation of the rigid Lsr2 filament on extended DNA by 15-min incubation. Then, 200 nM DNase I in 10 mM Tris–HCl and 50 mM KCl, pH 7.5, buffer conditions (without or with 10 mM $MgCl_2$, respectively) was introduced, and the rate of DNA digestion was monitored. Figure 4A shows a typical experiment in the absence of $MgCl_2$, where only 10% of Lsr2 nucleoprotein filament tethers were digested within 10 min, whereas in the case of unprotected DNA in the same buffer condition, all tethers were cleaved within 2 min. Similar results were also observed in the presence of 10 mM $MgCl_2$. The slight increase in the digestion rate in 10 mM $MgCl_2$ could be explained by increased activity of DNase I in the presence of $MgCl_2$. Although only one experiment in each condition was shown in Figure 4A and B for clarity, such experiments were repeated at least three times in each buffer condition with similar results (Supplementary Figure S5). Overall, these results indicate that extended DNA covered by rigid Lsr2 filament is sufficient to strongly restrict DNA access by DNase I. As DNase I digestion of DNA only requires access to 6 bp of exposed DNA, these results imply that DNA covered by Lsr2 filament should be able to block the access to DNA by RNA polymerase, which requires ~70 bp of exposed DNA (42).

DISCUSSION

Structural implication of cooperative Lsr2 binding on extended DNA

This work shows *M. tuberculosis* Lsr2 protein cooperatively binds to extended DNA resulting in a rigid Lsr2–DNA complex that has a much higher bending stiffness than a typical B-form DNA. A cooperative binding on an extended linear DNA track implies formation of a nucleoprotein filament. Results in Figure 1B also showed that the fully covered rigid Lsr2 nucleoprotein filament has similar contour length to that of a naked DNA, suggesting that the formation of Lsr2 filament on extended DNA does not cause significant distortion of the DNA backbone. Based on these observations, we propose that Lsr2 wraps around DNA and buries DNA inside. This also explains why DNA covered by Lsr2 can drastically restrict DNA accessibility. All these observations have been found in our previous studies of H-NS-like proteins in Gram-negative bacteria (21,31), further highlighting the universality and potential physiological importance of such nucleoprotein filamentous structures. Here, we want to emphasize that the cooperative nucleoprotein filament formation by Lsr2 is not artificially triggered by a forced extended DNA conformation, as on short length scale comparable with the persistence length of DNA (~50 nm or 150 bp), DNA is always locally extended in the absence of tensile force because of the intrinsic DNA-bending rigidity (43).

Mechanism of Lsr2-mediated physical DNA organization

Other than the DNA-stiffening effect of Lsr2 at high DNA tension, we also showed that Lsr2 caused DNA folding at low DNA tension, which was complemented with the observed aggregation of Lsr2–DNA complexes in our AFM imaging experiments where no tension was applied to the DNA molecules. This is consistent with previous AFM studies that showed Lsr2 can bridge DNA (30). As such, we see that DNA tension can regulate the observed DNA-binding properties of Lsr2; high DNA tension (high DNA stretching force) favours DNA-stiffening mode, whereas low DNA tension favours DNA folding. In cell, many DNA processing motors, such as DNA or RNA polymerases, can exert force on DNA up to 30 pN (44–46), whereas the occasional interaction between nucleoid and cell membrane may also impose a certain mechanical constraint on the chromosomal DNA (47). This suggests the chromosomal DNA is always under a variation of tension and mechanical stress, which potentially affects protein–DNA interactions and thus brings forth the physiological relevancy in how Lsr2 organizes DNA under force constraint.

Although it is likely high-DNA tension (>10 pN) applied during protein introduction prevents the DNA from Lsr2 folding, we cannot exclude the possibility that DNA tension and thus a more extended DNA conformation might preferentially select binding of an Lsr2 species that stiffens DNA. A relaxed DNA conformation at low DNA tension may then allow dominant binding by another Lsr2 species that causes DNA folding. This scenario is possible given the solution oligomeric nature of Lsr2 (30,48) and can also explain the observation of tension-regulated DNA stiffening and folding by Lsr2.

In addition, as revealed in our previous studies on StpA and MvaT (21,31), DNA folding and DNA stiffening do not necessarily exclude each other. In fact, DNA folding can be mediated by DNA-binding proteins in numerous pathways. The StpA nucleoprotein filaments, for an example, can mediate DNA bridging when this filament meets another naked DNA segment in low $MgCl_2$ concentration, whereas higher-ordered DNA organization occurs at higher $MgCl_2$ concentration through interactions between StpA nucleoprotein filaments (31). Similarly, the MvaT nucleoprotein filaments were able to mediate complex higher-ordered DNA organization (21). These similarities suggest that DNA folding by Lsr2 may also be mediated by locally formed Lsr2 nucleoprotein filaments that interact with each other. Future studies using systematic Lsr2 mutations to isolate its individual DNA organization mechanism will help to address this question.

Implications of Lsr2 DNA-binding properties in its physiological functions

The results from this work provide a platform to study how Lsr2 may perform its functions *in vivo*. Lsr2 DNA-folding ability suggests that it may potentially play an important role in DNA organization in *M. tuberculosis*. This is seen in many cases of DNA-folding bacterial NAPs that are involved in chromosomal DNA packaging (49–51). In particular, *E. coli* H-NS was shown highly localized in *E. coli* chromosome (4,52), and deletion of H-NS results in global reorganization of the *E. coli* chromosome DNA (4). Lsr2 prefers binding to AT-rich DNA sequences, and its binding sites are correlated with low CG-content segments of the genomic DNA (22). We also performed single-DNA stretching experiments on truncated fragments of λ-DNA; a 19 kb 57% CG-rich fragment and a 15 kb 54% AT-rich fragment and found no change in Lsr2 DNA-binding modes on either fragments (see Supplementary Figure S6). We still observed DNA-stiffening effects of Lsr2 whether with high-CG– or -AT–rich fragments, whereas in both cases, Lsr2 DNA folding was induced at low force. This suggests DNA sequence has no significant effect on how Lsr2 organizes DNA but rather tunes its DNA-binding affinity as previously shown (22).

In addition, the resistance of the rigid Lsr2–DNA complexes to salt and pH within physiological range suggests Lsr2 may not take part in gene regulatory regions that are pH and salt sensitive. This is contrary to Gram-negative H-NS, which was shown to be sensitive to salt and pH changes (24,53) and involved in the regulation of salt-sensitive proU operon (54). The differential response of Lsr2 and H-NS to pH might be due to the fact that Lsr2 is more basic than H-NS with a predicted pI of 10.69 compared with 5.25 for H-NS; therefore, it is more likely to bind negatively charged DNA at the range of pH tested (pH 6.8–8.8). On the other hand, the rigid Lsr2–DNA complexes are shown to be more sensitive to temperature than salt or pH as indicated by a drop in Lsr2 DNA-stiffening effect at 37°C. This shows certain similarity to H-NS, which is also a temperature sensor (24,53), although H-NS has a much drastic response to temperature. This suggests that Lsr2 may potentially be involved in regulating operons that are temperature sensitive. Transcription of *lsr2* was also found to be upregulated at high temperatures (55).

The emerging discovery of bacterial NAPs (H-NS, StpA, MvaT and Dan) nucleoprotein filament structures is intriguing (21,24,31,56). Strikingly, all of these proteins are known to involve in regulating DNA transcriptions, mainly repressive actions. For example, H-NS is a known global gene silencer (7), StpA represses RpoS (sigma 38) regulon (57) and loss of MvaT expression resulted in higher expression of Pf4 genes (58). As all of these proteins form similar rigid nucleoprotein filaments, it suggests that such nucleoprotein filaments may play an important role in repressing gene expressions. Given the numerous similarities between Lsr2 and H-NS family proteins in Gram-negative bacteria as revealed from this work, the proposed rigid Lsr2 nucleoprotein filament has the potential to be the structural basis for its gene-silencing function.

In summary, we show that Lsr2 cooperatively binds to extended DNA and covers the DNA possibly through formation of a rigid nucleoprotein filament. This proposed Lsr2 nucleoprotein filament, in addition to providing a potential structural basis for its gene-silencing function, may also mediate physical DNA organization in *M. tuberculosis* based on its DNA-folding capability. Most importantly, the extensive similarities in the DNA-binding properties between *M. tuberculosis* Lsr2 and H-NS family proteins in Gram-negative bacteria are consistent with the functional similarity reported in previous studies (11,22,59). Taken all of these together, our results provide additional evidence supporting that Lsr2 is a Gram-positive member of H-NS family protein from a DNA micro-mechanics perspective.

SUPPLEMENTARY DATA

Supplementary Data are available at NAR Online: Supplementary Figures 1–6, Supplementary Methods and Supplementary Reference [60].

ACKNOWLEDGEMENTS

The authors thank Dr Adam Yuan and the Mechanobiology Institute, Singapore Protein Expression Facility for protein expression and purification services. They also thank Dr Li Yang and Li Ang from Bruker Singapore for their technical assistance and service

rendered in operating Bruker FastScan AFM for our AFM imaging experiments.

FUNDING

National Research Foundation of Singapore through the Mechanobiology Institute at National University of Singapore (to J.Y.); Canadian Institutes of Health Research (CIHR) [MOP-15107 to J.L.]. Funding for open access charge: National Research Foundation of Singapore through the Mechanobiology Institute at National University of Singapore (to J.Y.).

Conflict of interest statement. None declared.

REFERENCES

1. Azam,T.A. and Ishihama,A. (1999) Twelve species of the nucleoid-associated protein from *Escherichia coli*-sequence recognition specificity and DNA binding affinity. *J. Biol. Chem.*, **274**, 33105–33113.
2. Browning,D.F., Grainger,D.C. and Busby,S.J. (2010) Effects of nucleoid-associated proteins on bacterial chromosome structure and gene expression. *Curr. Opin. Microbiol.*, **13**, 773–780.
3. Dillon,S.C. and Dorman,C.J. (2010) Bacterial nucleoid-associated proteins, nucleoid structure and gene expression. *Nat. Rev. Microbiol.*, **8**, 185–195.
4. Wang,W., Li,G.W., Chen,C., Xie,X.S. and Zhuang,X. (2011) Chromosome organization by a nucleoid-associated protein in live bacteria. *Science*, **333**, 1445–1449.
5. Azam,T.A., Iwata,A., Nishimura,A., Ueda,S. and Ishihama,A. (1999) Growth phase-dependent variation in protein composition of the *Escherichia coli* nucleoid. *J. Bacteriol.*, **181**, 6361–6370.
6. Zhang,A.X., Rimsky,S., Reaban,M.E., Buc,H. and Belfort,M. (1996) *Escherichia coli* protein analogs StpA and H-NS: regulatory loops, similar and disparate effects on nucleic acid dynamics. *EMBO J.*, **15**, 1340–1349.
7. Dorman,C.J. (2007) H-NS, the genome sentinel. *Nat. Rev. Microbiol.*, **5**, 157–161.
8. Hommais,F., Krin,E., Laurent-Winter,C., Soutourina,O., Malpertuy,A., Le Caer,J.P., Danchin,A. and Bertin,P. (2001) Large-scale monitoring of pleiotropic regulation of gene expression by the prokaryotic nucleoid-associated protein, H-NS. *Mol. Microbiol.*, **40**, 20–36.
9. White-Ziegler,C.A. and Davis,T.R. (2009) Genome-wide identification of H-NS-controlled, temperature-regulated genes in *Escherichia coli* K-12. *J. Bacteriol.*, **191**, 1106–1110.
10. Lucchini,S., Rowley,G., Goldberg,M.D., Hurd,D., Harrison,M. and Hinton,J.C. (2006) H-NS mediates the silencing of laterally acquired genes in bacteria. *PLoS Pathog.*, **2**, e81.
11. Gordon,B.R., Imperial,R., Wang,L., Navarre,W.W. and Liu,J. (2008) Lsr2 of *Mycobacterium* represents a novel class of H-NS-like proteins. *J. Bacteriol.*, **190**, 7052–7059.
12. Shi,X.L. and Bennett,G.N. (1994) Plasmids bearing hfq and the hns-like gene stpa complement hns mutants in modulating arginine decarboxylase gene-expression in *Escherichia-coli*. *J. Bacteriol.*, **176**, 6769–6775.
13. Zhang,A.X. and Belfort,M. (1992) Nucleotide-sequence of a newly-identified *Escherichia coli* gene, stpa, encoding an H-Ns-like protein. *Nucleic Acids Res.*, **20**, 6735–6735.
14. Castang,S. and Dove,S.L. (2010) High-order oligomerization is required for the function of the H-NS family member MvaT in *Pseudomonas aeruginosa*. *Mol. Microbiol.*, **78**, 916–931.
15. Goyard,S. and Bertin,P. (1997) Characterization of BpH3, an H-NS-like protein in *Bordetella pertussis*. *Mol. Microbiol.*, **24**, 815–823.
16. Tendeng,C., Badaut,C., Krin,E., Gounon,P., Ngo,S., Danchin,A., Rimsky,S. and Bertin,P. (2000) Isolation and characterization of vicH, encoding a new pleiotropic regulator in *Vibrio cholerae*. *J. Bacteriol.*, **182**, 2026–2032.
17. Ueguchi,C., Seto,C., Suzuki,T. and Mizuno,T. (1997) Clarification of the dimerization domain and its functional significance for the *Escherichia coli* nucleoid protein H-NS. *J. Mol. Biol.*, **274**, 145–151.
18. Esposito,D., Petrovic,A., Harris,R., Ono,S., Eccleston,J.F., Mbabaali,A., Haq,I., Higgins,C.F., Hinton,J.C., Driscoll,P.C. *et al.* (2002) H-NS oligomerization domain structure reveals the mechanism for high order self-association of the intact protein. *J. Mol. Biol.*, **324**, 841–850.
19. Rimsky,S. (2004) Structure of the histone-like protein H-NS and its role in regulation and genome superstructure. *Curr. Opin. Microbiol.*, **7**, 109–114.
20. Dorman,C.J., Hinton,J.C. and Free,A. (1999) Domain organization and oligomerization among H-NS-like nucleoid-associated proteins in bacteria. *Trends Microbiol.*, **7**, 124–128.
21. Winardhi,R.S., Fu,W., Castang,S., Li,Y., Dove,S.L. and Yan,J. (2012) Higher order oligomerization is required for H-NS family member MvaT to form gene-silencing nucleoprotein filament. *Nucleic Acids Res.*, **40**, 8942–8952.
22. Gordon,B.R., Li,Y., Cote,A., Weirauch,M.T., Ding,P., Hughes,T.R., Navarre,W.W., Xia,B. and Liu,J. (2011) Structural basis for recognition of AT-rich DNA by unrelated xenogeneic silencing proteins. *Proc. Natl Acad. Sci. USA*, **108**, 10690–10695.
23. Dame,R.T., Wyman,C. and Goosen,N. (2000) H-NS mediated compaction of DNA visualised by atomic force microscopy. *Nucleic Acids Res.*, **28**, 3504–3510.
24. Liu,Y., Chen,H., Kenney,L.J. and Yan,J. (2010) A divalent switch drives H-NS/DNA-binding conformations between stiffening and bridging modes. *Genes Dev.*, **24**, 339–344.
25. Fang,F.C. and Rimsky,S. (2008) New insights into transcriptional regulation by H-NS. *Curr. Opin. Microbiol.*, **11**, 113–120.
26. Lim,C.J., Lee,S.Y., Kenney,L.J. and Yan,J. (2012) Nucleoprotein filament formation is the structural basis for bacterial protein H-NS gene silencing. *Sci. Rep.*, **2**, 509.
27. Walthers,D., Li,Y., Liu,Y., Anand,G., Yan,J. and Kenney,L.J. (2011) *Salmonella enterica* response regulator SsrB relieves H-NS silencing by displacing H-NS bound in polymerization mode and directly activates transcription. *J. Biol. Chem.*, **286**, 1895–1902.
28. Rowbury,R.J. (1997) Regulatory components, including integration host factor, CysB and H-NS, that influence pH responses in *Escherichia coli*. *Lett. Appl. Microbiol.*, **24**, 319–328.
29. Lin,J., Chen,H., Droge,P. and Yan,J. (2012) Physical organization of DNA by multiple non-specific DNA-binding modes of integration host factor (IHF). *PLoS One*, **7**, e49885.
30. Chen,J.M., Ren,H., Shaw,J.E., Wang,Y.J., Li,M., Leung,A.S., Tran,V., Berbenetz,N.M., Kocincova,D., Yip,C.M. *et al.* (2008) Lsr2 of *Mycobacterium tuberculosis* is a DNA-bridging protein. *Nucleic Acids Res.*, **36**, 2123–2135.
31. Lim,C.J., Whang,Y.R., Kenney,L.J. and Yan,J. (2012) Gene silencing H-NS paralogue StpA forms a rigid protein filament along DNA that blocks DNA accessibility. *Nucleic Acids Res.*, **40**, 3316–3328.
32. Dame,R.T., Luijsterburg,M.S., Krin,E., Bertin,P.N., Wagner,R. and Wuite,G.J.L. (2005) DNA bridging: a property shared among H-NS-like proteins. *J. Bacteriol.*, **187**, 1845–1848.
33. Yan,J., Skoko,D. and Marko,J. (2004) Near-field-magnetic-tweezer manipulation of single DNA molecules. *Phys. Rev. E Stat. Nonlin. Soft. Matter Phys.*, **70**, 011905.
34. Wang,H.D., Bash,R., Yodh,J.G., Hager,G.L., Lohr,D. and Lindsay,S.M. (2002) Glutaraldehyde modified mica: a new surface for atomic force microscopy of chromatin. *Biophys. J.*, **83**, 3619–3625.
35. Fu,H., Freedman,B.S., Lim,C.T., Heald,R. and Yan,J. (2011) Atomic force microscope imaging of chromatin assembled in *Xenopus laevis* egg extract. *Chromosoma*, **120**, 245–254.
36. Yan,J. and Marko,J.F. (2003) Effects of DNA-distorting proteins on DNA elastic response. *Phys. Rev. E Stat. Nonlin. Soft. Matter. Phys.*, **68**, 011905.
37. Marko,J.F. and Siggia,E.D. (1995) Stretching DNA. *Macromolecules*, **28**, 8759–8770.
38. Smith,S.B., Finzi,L. and Bustamante,C. (1992) Direct mechanical measurements of the elasticity of single DNA molecules by using magnetic beads. *Science*, **258**, 1122–1126.

39. Hill,A.V. (1910) The possible effects of the aggregation of the molecules of haemoglobin on its dissociation curves. *J. Physiol.*, **40**, iv–vii.
40. Colangeli,R., Helb,D., Vilcheze,C., Hazbon,M.H., Lee,C.G., Safi,H., Sayers,B., Sardone,I., Jones,M.B., Fleischmann,R.D. *et al.* (2007) Transcriptional regulation of multi-drug tolerance and antibiotic-induced responses by the histone-like protein Lsr2 in *M. tuberculosis*. *PLoS Pathog.*, **3**, e87.
41. Colangeli,R., Haq,A., Arcus,V.L., Summers,E., Magliozzo,R.S., McBride,A., Mitra,A.K., Radjainia,M., Khajo,A., Jacobs,W.R. Jr *et al.* (2009) The multifunctional histone-like protein Lsr2 protects mycobacteria against reactive oxygen intermediates. *Proc. Natl Acad. Sci. USA*, **106**, 4414–4418.
42. Talkington,C. and Pero,J. (1979) Distinctive nucleotide sequences of promoters recognized by RNA polymerase containing a phage-coded "sigma-like" protein. *Proc. Natl Acad. Sci. USA*, **76**, 5465–5469.
43. Doi,M. and Edwards,S.F. (1988) *The Theory of Polymer Dynamics*. Oxford University Press, USA, New York.
44. Wang,M.D., Schnitzer,M.J., Yin,H., Landick,R., Gelles,J. and Block,S.M. (1998) Force and velocity measured for single molecules of RNA polymerase. *Science*, **282**, 902–907.
45. Davenport,R.J., Wuite,G.J., Landick,R. and Bustamante,C. (2000) Single-molecule study of transcriptional pausing and arrest by *E. coli* RNA polymerase. *Science*, **287**, 2497–2500.
46. Maier,B., Bensimon,D. and Croquette,V. (2000) Replication by a single DNA polymerase of a stretched single-stranded DNA. *Proc. Natl Acad. Sci. USA*, **97**, 12002–12007.
47. Toro,E. and Shapiro,L. (2010) Bacterial chromosome organization and segregation. *Cold Spring Harb. Perspect. Biol.*, **2**, a000349.
48. Summers,E.L., Meindl,K., Uson,I., Mitra,A.K., Radjainia,M., Colangeli,R., Alland,D. and Arcus,V.L. (2012) The structure of the oligomerization domain of Lsr2 from *Mycobacterium tuberculosis* reveals a mechanism for chromosome organization and protection. *PLoS One*, **7**, e38542.
49. Kim,J., Yoshimura,S.H., Hizume,K., Ohniwa,R.L., Ishihama,A. and Takeyasu,K. (2004) Fundamental structural units of the *Escherichia coli* nucleoid revealed by atomic force microscopy. *Nucleic Acids Res.*, **32**, 1982–1992.
50. Kaidow,A., Wachi,M., Nakamura,J., Magae,J. and Nagai,K. (1995) Anucleate cell production by *Escherichia coli* delta hns mutant lacking a histone-like protein, H-NS. *J. Bacteriol.*, **177**, 3589–3592.
51. Ghatak,P., Karmakar,K., Kasetty,S. and Chatterji,D. (2011) Unveiling the role of Dps in the organization of mycobacterial nucleoid. *PLos One*, **6**, e16019.
52. Azam,T.A., Hiraga,S. and Ishihama,A. (2000) Two types of localization of the DNA-binding proteins within the *Escherichia coli* nucleoid. *Genes Cells*, **5**, 613–626.
53. Amit,R., Oppenheim,A.B. and Stavans,J. (2003) Increased bending rigidity of single DNA molecules by H-NS, a temperature and osmolarity sensor. *Biophys. J.*, **84**, 2467–2473.
54. Lucht,J.M., Dersch,P., Kempf,B. and Bremer,E. (1994) Interactions of the nucleoid-associated DNA-binding protein H-NS with the regulatory region of the osmotically controlled proU operon of *Escherichia coli*. *J. Biol. Chem.*, **269**, 6578–6578.
55. Stewart,G.R., Wernisch,L., Stabler,R., Mangan,J.A., Hinds,J., Laing,K.G., Young,D.B. and Butcher,P.D. (2002) Dissection of the heat-shock response in *Mycobacterium tuberculosis* using mutants and microarrays. *Microbiology*, **148**, 3129–3138.
56. Lim,C.J., Lee,S.Y., Teramoto,J., Ishihama,A. and Yan,J. (2012) The nucleoid-associated protein Dan organizes chromosomal DNA through rigid nucleoprotein filament formation in *E. coli* during anoxia. *Nucleic Acids Res.*, **41**, 746–753.
57. Lucchini,S., McDermott,P., Thompson,A. and Hinton,J.C. (2009) The H-NS-like protein StpA represses the RpoS (sigma 38) regulon during exponential growth of *Salmonella typhimurium*. *Mol. Microbiol.*, **74**, 1169–1186.
58. Castang,S. and Dove,S.L. (2012) Basis for the essentiality of H-NS family members in *Pseudomonas aeruginosa*. *J. Bacteriol.*, **194**, 5101–5109.
59. Gordon,B.R., Li,Y., Wang,L., Sintsova,A., van Bakel,H., Tian,S., Navarre,W.W., Xia,B. and Liu,J. (2010) Lsr2 is a nucleoid-associated protein that targets AT-rich sequences and virulence genes in *Mycobacterium tuberculosis*. *Proc. Natl Acad. Sci. USA*, **107**, 5154–5159.
60. Fu,H., Chen,H., Marko,J.F. and Yan,J. (2010) Two distinct overstretched DNA states. *Nucleic Acids Res.*, **38**, 5594–5600.